Real-Scale Integral Valorization of Waste Orange Peel via Hydrodynamic Cavitation

Authors:

Francesco Meneguzzo, Cecilia Brunetti, Alexandra Fidalgo, Rosaria Ciriminna, Riccardo Delisi, Lorenzo Albanese, Federica Zabini, Antonella Gori, Luana Beatriz dos Santos Nascimento, Anna De Carlo, Francesco Ferrini, Laura M. Ilharco, Mario Pagliaro

Date Submitted: 2019-11-24

Keywords: polyphenols, pectin, orange waste, green extraction, hydrodynamic cavitation, food waste, flavanones, d-limonene, biomethane

Abstract:

Waste orange peel represents a heavy burden for the orange juice industry, estimated in several million tons per year worldwide; nevertheless, this by-product is endowed with valuable bioactive compounds, such as pectin, polyphenols, and terpenes. The potential value of the waste orange peel has stimulated the search for extraction processes, alternative or complementary to landfilling or to the integral energy conversion. This study introduces controlled hydrodynamic cavitation as a new route to the integral valorization of this by-product, based on simple equipment, speed, effectiveness and efficiency, scalability, and compliance with green extraction principles. Waste orange peel, in batches of several kg, was processed in more than 100 L of water, without any other raw materials, in a device comprising a Venturi-shaped cavitation reactor. The extractions of pectin (with a remarkably low degree of esterification), polyphenols (flavanones and hydroxycinnamic acid derivatives), and terpenes (mainly d-limonene) were effective and efficient (high yields within a few min of process time). The biomethane generation potential of the process residues was determined. The achieved results proved the viability of the proposed route to the integral valorization of waste orange peel, though wide margins exist for further improvements.

Record Type: Published Article

Submitted To: LAPSE (Living Archive for Process Systems Engineering)

Citation (overall record, always the latest version):	LAPSE:2019.1170
Citation (this specific file, latest version):	LAPSE:2019.1170-1
Citation (this specific file, this version):	LAPSE:2019.1170-1v1

DOI of Published Version: https://doi.org/10.3390/pr7090581

processes

MDPI

Article

Real-Scale Integral Valorization of Waste Orange Peel via Hydrodynamic Cavitation

Francesco Meneguzzo [1,*], Cecilia Brunetti [1], Alexandra Fidalgo [2], Rosaria Ciriminna [3], Riccardo Delisi [4], Lorenzo Albanese [1], Federica Zabini [1], Antonella Gori [5], Luana Beatriz dos Santos Nascimento [5], Anna De Carlo [1,5], Francesco Ferrini [1,5], Laura M. Ilharco [2] and Mario Pagliaro [3]

1 Institute for Bioeconomy, National Research Council, 10 Via Madonna del Piano, I-50019 Sesto Fiorentino (FI), Italy
2 Centro de Química-Física Molecular and IN-Institute of Nanoscience and Nanotechnology, Instituto Superior Técnico, University of Lisboa, Complexo I, Avenida Rovisco Pais 1, 1649-004 Lisboa, Portugal
3 Istituto per lo Studio dei Materiali Nanostrutturati, CNR, via U. La Malfa 153, 90146 Palermo, Italy
4 Renovo Biochemicals srl, 1 Via P. Verri, I-46100 Mantova (MN), Italy
5 Department of Agriculture, Food, Environment, and Forestry (DAGRI), University of Florence, Viale delle Idee 30, I-50019 Sesto Fiorentino (FI), Italy
* Correspondence: francesco.meneguzzo@cnr.it; Tel.: +39-392-985-0002

Received: 28 July 2019; Accepted: 29 August 2019; Published: 2 September 2019

Abstract: Waste orange peel represents a heavy burden for the orange juice industry, estimated in several million tons per year worldwide; nevertheless, this by-product is endowed with valuable bioactive compounds, such as pectin, polyphenols, and terpenes. The potential value of the waste orange peel has stimulated the search for extraction processes, alternative or complementary to landfilling or to the integral energy conversion. This study introduces controlled hydrodynamic cavitation as a new route to the integral valorization of this by-product, based on simple equipment, speed, effectiveness and efficiency, scalability, and compliance with green extraction principles. Waste orange peel, in batches of several kg, was processed in more than 100 L of water, without any other raw materials, in a device comprising a Venturi-shaped cavitation reactor. The extractions of pectin (with a remarkably low degree of esterification), polyphenols (flavanones and hydroxycinnamic acid derivatives), and terpenes (mainly *d*-limonene) were effective and efficient (high yields within a few min of process time). The biomethane generation potential of the process residues was determined. The achieved results proved the viability of the proposed route to the integral valorization of waste orange peel, though wide margins exist for further improvements.

Keywords: biomethane; *d*-limonene; flavanones; food waste; green extraction; hydrodynamic cavitation; orange waste; pectin; polyphenols

1. Introduction

Accounting for 61% of the world's citrus fruit production [1], the global production of sweet orange (*Citrus sinensis* (L.) Osbeck) in 2017–2018 exceeded 47 million tons, 36% of which (17 million tons) was used in orange juice production [2]. Production for 2018–2019 was predicted to grow by another 4.2 million metric tons. Large amounts of by-products, estimated at a level between 50% and 60% of the harvest, consist of discarded fruits, peels, and seeds. Effective technologies to upgrade the value of these said by-products, which have been so far mostly dealt with as waste, are of direct and significant relevance to all orange-growing countries and regions, including Brazil, Florida, India, South Africa, Spain, Turkey, and Italy [3]. Waste orange peel (WOP), in particular, contains

highly valuable bioproducts, such as carbohydrate polymers (cellulose, hemicellulose, and pectin), polyphenols (including naringin and hesperidin), and essential oils (mostly *d*-limonene) [1].

The affordable, large-scale extraction and valorization of these compounds would also result in the size reduction of the relevant waste stream, thus relieving the environmental burden related to the still frequent disposal of the WOP in landfills or saving valuable biocompounds before the energy conversion of the residues. Anaerobic co-digestion, carried out after the extraction and removal of *d*-limonene, an inhibitory compound, was assessed as the most environmentally performing technique for the energetic valorization of WOP by means of biogas generation [3]. Indeed, the latter practice has been increasingly applied in some orange intensive production areas, such as Sicily.

Extracted from the orange peel prior to squeezing via a mechanical process (a jet of water breaking the oil-containing glands), orange essential oil (EO) mostly contains *d*-limonene [4], a monoterpene whose average content in *Citrus sinensis* fruit peels is 3.8 wt % on a dry weight basis [5,6]. This molecule was first used in the 1950s as a bio-solvent and today is the main ingredient of numerous bio-based functional products whose demand is rapidly growing [6]. In the early 1990s, its plant anti-fungal and antibacterial properties were first identified [7], leading to the development and utilization of biopesticide formulations, in which orange oil, and thus *d*-limonene, was the active ingredient [8]. After the discovery of its natural ozone scavenging properties, in 2005 *d*-limonene was proposed as an effective adjuvant in preventive therapies against asthma [9]. Due to its broad spectrum of antimicrobial, antioxidant, and anti-inflammatory properties, *d*-limonene is now used in many cosmetic and nutraceutical applications, as well as an anti-spoilage additive in food [10].

Pectin is currently mostly produced from citrus peels (56% from lemons, 30% from limes, and 13% from oranges) and, to a lesser extent (14%), from apple pomace [11], and it is the most valued natural hydrocolloid [12]. Since the early 2000s, it was established that pectin has various beneficial effects on health and nutrition as a dietary and prebiotic fiber, with numerous applications in the food, feed, cosmetic, medical, and pharmaceutical industries [12,13]. Effectively reducing the interfacial surface tension between the oil and water phases, pectin is also an excellent emulsifier and emulsion stabilizer [14,15]. Orange-extracted pectin powder added to an oil-in-water sub-micron size emulsion (20% *w/w* of orange oil), prepared with a standard homogenizer, exhibited substantial stability up to at least 30 days from preparation [14].

In the last fifteen years, numerous green chemistry processes were applied to extract the valued components of WOP resulting from the orange juice industry. WOP is a potential source of fat (oleic, linoleic, linolenic, palmitic, and stearic acids, and phytosterols), mono- and disaccharides (glucose, fructose, and sucrose), organic acids (mainly citric, malic, and tartaric, but also benzoic, oxalic, and succinic acids), polysaccharides (cellulose, hemicellulose, and pectin), enzymes (pectinesterase, phosphatase, and peroxidase), flavonoids (hesperidin, naringin, and narirutin), terpenes (*d*-limonene, linalool, and myrcene), and pigments (carotenoids and xanthophylls).

A few years ago, solvent-free extraction processes using microwave and ultrasound techniques were successfully applied to obtain essential oils, polyphenols, and pectin through microwave hydrothermal processing [16]. Promising results were achieved using solar-driven vapor steam distillation, to obtain valued pectin, terpenes, and biophenols [17], as well as employing a solvent-free process based on microwave distillation, hydrodiffusion, and gravity [13].

Hydrodynamic cavitation (HC) is generally achieved via pumping a liquid through one or more constrictions of suitable geometry, such as Venturi tubes and orifice plates. Controlled HC results in the generation, growth, and collapse of microbubbles due to pressure variations in the liquid flow [18]. The increase in kinetic energy at the constriction occurs at the expense of pressure, leading to the generation of microbubbles and nanobubbles, which subsequently collapse under pressure recovery downstream of the constriction [19]. The violent collapse of the cavitation bubbles results in the generation of localized hot spots endowed with extremely high-energy density [20,21], highly reactive free radicals, and turbulence, which can result in the intensification of various physical/chemical phenomena. These include wastewater remediation and enhancement of biogas generation [22–24],

preparation of nanoemulsions, biodiesel synthesis, water disinfection, and nanoparticle synthesis [25], among others.

In the recent past, cavitation has emerged as a green extraction technology for natural products, reducing process time and energy consumption, while achieving higher extraction yields, as well as a useful tool for the intensification of food and pharmaceutical processes [25,26]. The growing variety of applications has also stimulated the development of other promising arrangements, such as those based on rotating parts [27] and variants of fixed constrictions based, for example, on vortex dynamics [28], which are in the process of proving the respective affordability and straightforward scalability.

Real-scale applications of cavitation are quickly spreading in the food and beverage industries, including the processing of food waste [29]. Again, the HC processing of vegetable raw materials, such as grains and hops for beer-brewing [30,31] or plant leaves [32], and its application to the extraction of bioactive compounds [27], offer distinct advantages, such as shorter process times, higher energy efficiency and yields, and enhanced extraction rates. When compared with both conventional techniques and newer ones, including acoustic cavitation sustained by ultrasound irradiation, the HC-based processes showed superior performance, due to enhanced process yields and straightforward scalability [18,33].

HC-based techniques appear as natural candidates for applications to the valorization of WOP. Nevertheless, to the best of our knowledge, no studies have been reported so far on the application of hydrodynamic cavitation processes to extract the valued components of waste orange peel. This study reports the first results concerning a novel route to valorize WOP based on criteria of effectiveness, reliability, efficiency, and affordability. The starting idea was that waste orange peel contains EOs, water-soluble pectin, and polyphenols, which can be transferred to the aqueous phase. In particular, the EOs could form oil-in-water emulsions, stabilized by the presence of pectin. All this, carried out by means of HC processes and without additives, as elucidated in Section 2.2.

After the HC-based extraction process, the liquid phase could be used as such to functionalize foods and beverages, affecting both the nutraceutical properties and the shelf life. The residual WOP solid fraction, mostly composed of cellulose and hemicellulose and deprived of inhibitory compounds, such as the EOs, could be effectively used to produce biogas in an anaerobic digester, and the resulting digestate used as a soil amendant or easily converted into biochar or hydrochar [34,35].

2. Materials and Methods

2.1. HC Device and Processes

Figure 1 shows the experimental device implementing the HC-based process, including a closed hydraulic loop (total volume capacity around 230 L) and a centrifugal pump (Lowara, Vicenza, Italy, model ESHE 50-160/ 75, with 7.5 kW nominal mechanical power and rotation speed of 2900 rpm). The processes were carried out at atmospheric pressure (open plant).

Such a device was used in past studies, to carry out innovative beer-brewing [30,31,36,37], for which application an industrial-level plant (2000 L) was developed [38], to enhance biochar properties [39], and in the solvent-free extraction of bioactive compounds, namely polyphenols and flavonoids, from the leaves of silver fir plants [32]. The geometry of the Venturi-shaped cavitation reactor was defined and graphically represented in a previous study [40]: the reactor was circular, the throat diameter 2.4 cm, the convergence angle 22.61°, and the divergent angle 6.4°. Due to the diameter of the pipe at the level of 10.16 cm, the lengths of the convergent and divergent sections were 11 cm and 43 cm, respectively.

Venturi-shaped cavitation reactors were shown to outperform other reactors based on fixed constrictions, such as orifice plates, in the treatment of viscous food liquids [33]. This superiority especially holds with liquids containing solid particles, as well as for the inactivation of spoilage microorganisms [40], and the creation of oil-in-water stable nanoemulsions [41], all these features being relevant to the processes under study.

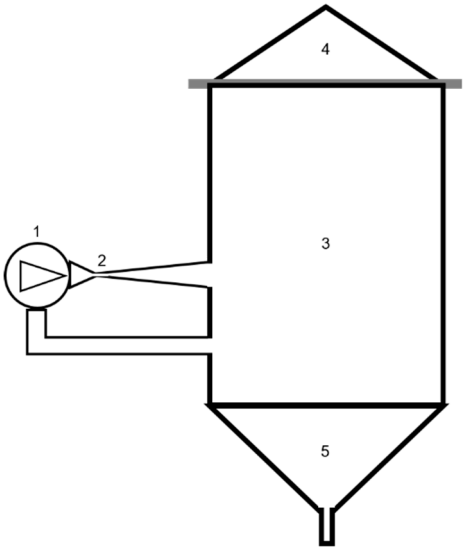

Figure 1. Experimental hydrodynamic cavitation (HC)-based installation. (1) Centrifugal pump, (2) HC reactor, (3) main vessel, (4) cover, (5) discharge.

In case of a fixed mechanical constriction, such as the Venturi-shaped HC reactor shown in Figure 1, the liquid velocity and static pressure are regulated by Bernoulli's equation [20], i.e., the conservation of the mechanical energy for a moving fluid is represented by Equation (1):

$$P_1 + \rho v_1^2/2 + \rho g h_1 = P_2 + \rho v_2^2/2 + \rho g h_2 \quad (1)$$

where P_1 and P_2 ($N \cdot m^{-2}$) are the upstream pressure and the pressure at the nozzle, respectively, ρ ($kg \cdot m^{-3}$) is the liquid density, v_1 and v_2 ($m \cdot s^{-1}$) are the fluid speed upstream and through the nozzle, respectively, h_1 and h_2 (m) are the heights of the fluid, and g ($m \cdot s^{-2}$) is gravity. The third term at each side of Equation (1) represents the specific potential energy, while the second term represents the specific kinetic energy. Assuming equal heights, the pressure drop ($P_2 < P_1$) arises at the reactor's nozzle because of the fluid acceleration due to mass conservation ($v_2 > v_1$). Whenever P_2 drops below the vapor pressure, at a certain temperature level, local evaporation occurs and vapor bubbles are generated.

Theoretical and experimental evidence has grown about the unique physical (mechanical and thermal) phenomena occurring at the scale of the collapsing cavitation bubbles [20,21], and the chemical phenomena, such as water splitting and generation of powerful oxidants (e.g., OH·hydroxyl radicals) [21,24]. However, the concentration of oxidizing compounds, which could be harmful in food processes, was found to be quite limited in the absence of specific additives [42,43].

Despite the inherent complexity of the physicochemical processes associated with cavitation, for fixed constrictions, a widely used dimensionless quantity, named the cavitation number (σ), can be used to characterize the cavitation intensity in a flow system in terms of easily measurable physical quantities. Its representativeness holds in most of the relatively simple HC reactors, such as Venturi tubes and orifice plates [20], and is related to the cavitational intensity, with cavitation generally arising for $\sigma < 1$. The cavitation number is derived from Bernoulli's equation [44] and represents the ratio between the pressure drop needed to achieve vaporization and the specific kinetic energy at the cavitation inception section, as per Equation (2):

$$\sigma = (P_0 - P_v)/(0.5 \cdot \rho \cdot v_2^2) \quad (2)$$

where P_0 ($N \cdot m^{-2}$) is the average recovered pressure downstream of the cavitation reactor, such as a Venturi tube or an orifice plate, where cavitation bubbles collapse. Since the fluid was not pressurized, P_0 was assumed to be equal to the atmospheric pressure. P_v ($N \cdot m^{-2}$) is the liquid-vapor pressure,

which is a function of the average temperature for any given liquid. As in Equation (1), v_2 ($m \cdot s^{-1}$) is the flow velocity through the nozzle of the cavitation reactor and depends on the pump's inlet pressure. In this study, the cavitation number values were computed according to the available data, such as temperature and pump discharge; the latter was based on the consumed power, as explained in a previous study [30].

Under conditions easily achievable in Venturi-shaped reactors, developed cavitation with frequent and violent bubble collapses occurs within the range $0.1 < \sigma < 1$ and even at higher values in the presence of solid particles or dissolved gases [45,46]. In general, the lower the cavitation number, the more efficient the cavitation processes, at least down to the onset of chocked cavitation conditions (supercavitation), even though that regime is very efficient for disinfection purposes [47].

2.2. Orange Waste Samples and Tests

Two HC-based extraction tests were performed using WOP from organic fruits of *Citrus sinensis* (L.) Osbeck, 'Washington navel orange' variety, originating from Sicily, Italy. The first test (WOP1) was carried out in March 2017, with WOP from red oranges kindly provided by Ortogel S.p.A. (Caltagirone, Sicily, Italy), representing the wastes from their orange juice production line. This test was aimed at the extraction and analysis of pectin, as well as at assessing the biochemical methane potential of the process solid residues.

The second test (WOP2) was carried out in April 2019, using raw material peels manually discarded from oranges collected at a local organic farm in Ribera, Sicily, Italy. This test aimed at analyzing the extraction rate of bioactive compounds, such as polyphenols and EOs (terpenes).

In both tests, WOP was frozen immediately after collection, ground in ice (maximum linear size of 10 mm) to avoid the degradation of bioactive compounds, then pitched into the HC device and processed in tap water only. Table 1 shows the basic features of both tests.

Table 1. Basic features of the waste orange peel (WOP) extraction tests. The WOP mass is expressed in kg of fresh weight.

Test	Water Volume (L)	WOP Mass (kg)	Test Duration (min)	Temperature (°C)
WOP1	120	42	270	14.5–96
WOP2	147	6.38	127	18.5–80

In both tests, the HC device was not airtight, allowing volatile compounds to escape, thereby hindering the retention of terpenes in aqueous solution and affecting the EO extraction yields. Among monoterpenes, *d*-limonene is particularly volatile; for example, its fraction, extracted from hops during high temperature steps of the brewing process, could not be retained in finished beer [48,49].

The evolution of the temperature and the cavitation number are shown in Figure 2a for the test WOP1 and in Figure 2b for the test WOP2, along with the respective sampling points. No temperature control (i.e., no cooling step) was performed, thus the overall heating was the result of the balance between the mechanical energy supplied by the pump's impeller and the heat loss from the uninsulated device [36].

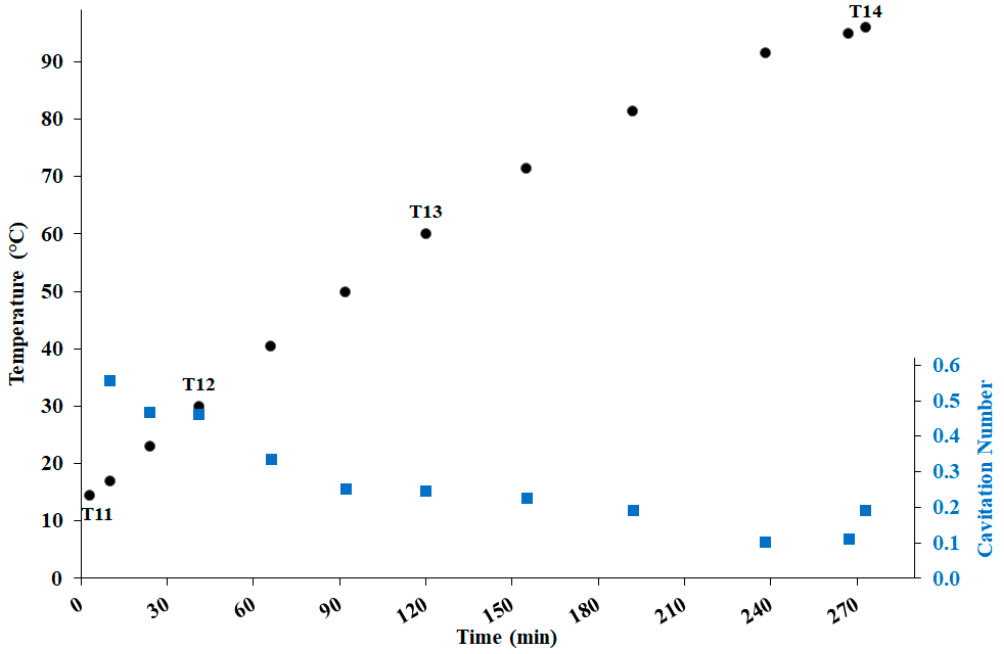

(**a**)

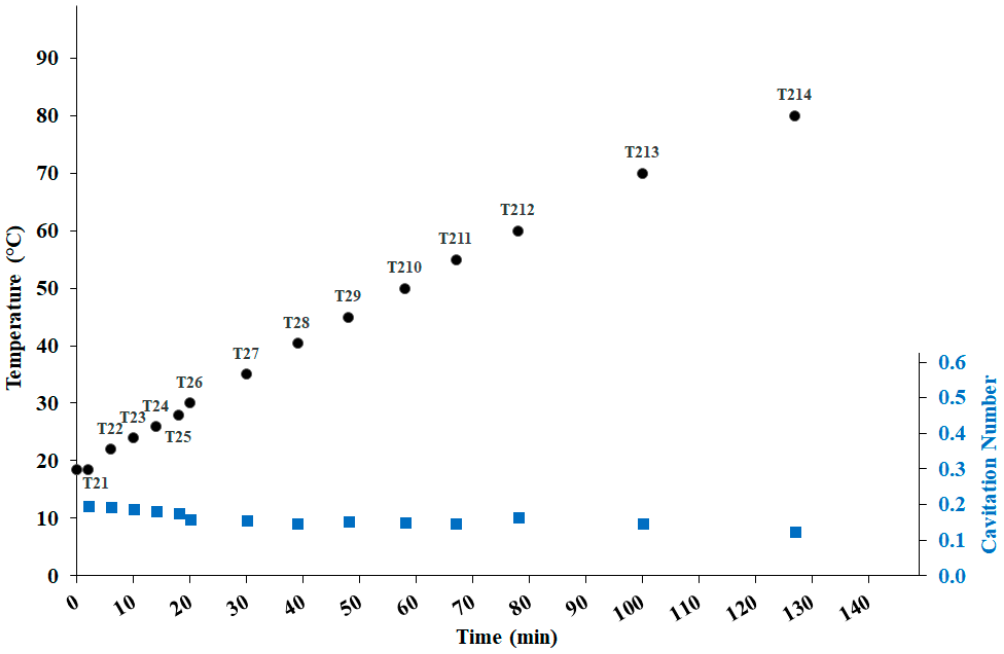

(**b**)

Figure 2. Evolution of the temperature and the cavitation number, along with sampling points (from T11 to T14 for WOP1 and from T21 to T214 for WOP2), in the two tests: (**a**) WOP1; (**b**) WOP2.

In the earlier phase of the WOP1 test (more than 30 min), the cavitation number was rather high (0.46 to 0.57), pointing to relatively poor cavitation performance. This behavior derived from the centrifugal pump running in a suboptimal regime (low consumed power) and was likely due to the high concentration of the raw material (28.6% *w*/*v*). Later, as the cavitation process caused the reduction of WOP particle size and promoted the extraction and solubilization of bioproducts, the cavitation number slowly decreased down to 0.1 at 91 °C (235 min). The final increase of σ up to 0.19 was

instead due to the strong friction induced by the high temperature, reducing the pump discharge and counteracting the effect of the increased vapor pressure.

Due to the suboptimal performance during the earlier phase of the WOP1 test, a substantially lower concentration of WOP was used for the WOP2 test (4.3% *w/v*), where the sampling was much more frequent in time. Indeed, in WOP2, the cavitation number was as low as 0.2 from the beginning, slowly decreasing in the first 20 min, then stabilizing around 0.15, and finally decreasing again down to 0.12 during the heating from 70 °C to 80 °C, as a result of the increasing vapor pressure. These levels of the cavitation number fell within the recommended range, found for brewing applications using the same device as in this study [30].

The specific energy consumed (electricity per kg of fresh WOP), limited to the range 18 to 80 °C for a heating of 10 °C, was on average 0.065 kWh/kg in WOP1 and 0.36 kWh/kg in WOP2. This outcome is the result of the higher water volume by 1.225 times and the lower content of raw material by 6.6 times in WOP2. However, the ratio of the specific energies (about 5.5) was lower than expected, based on the above-mentioned data, because the pump in WOP2 was more efficient (higher consumed power, by 1.2 times on average), thus the heating rate was higher and the heat loss from the uninsulated device was lower. The overall specific energy consumed at the end of the WOP1 and WOP2 tests was around 0.62 kWh/kg and 2.20 kWh/kg, respectively.

2.3. Experimental and Analytical Procedures

2.3.1. Biochemical Methane Generation Potential

The biochemical methane potential (BMP) of the solid residues obtained in the WOP1 test was evaluated using assays performed by a standard method [50]. In detail, vessel-shaped static reactors of 100 mL were filled in with a mixture consisting of a portion of the WOP1 solid residues (substrate) and an inoculum obtained from an existing biogas generation plant. Such inoculum included mesophilic bacteria and biomass with the following characteristics: moisture 94.2% (wet basis), ash 25.1%, volatile substance (VS) 69.1%, carbon content 41.7%, hydrogen content 5.1%, nitrogen content 2.3%, and sulfur content 0.5%, all such quantities being determined on a dry basis, unless otherwise stated. One vessel containing only the inoculum served as a blank test. The mass of both WOP1 process residues (substrate) and the inoculum was 0.6 g, thus the inoculum to substrate ratio was 1:1.

The vessels were kept warm at 38 °C in a thermal bath, and the daily volume of biogas generated was measured for 36 days, starting 15 days after the WOP1 test. Each measurement was performed in triplicate. The contribution of the WOP to the biogas production, normalized to the volatile substance's content, was estimated subtracting the average generation of the blank test of the WOP-containing vessels.

Based on each sample's composition, the theoretical biomethane generation potential (Th-BMP) and methane relative in the biogas were computed from Buswell's formulas [51]. The cumulative BMP attributed to the WOP1 solid residues was assessed on a daily basis, by multiplying the biogas generation by the methane content.

2.3.2. Pectin

Pectin extracted from citrus fruits is generally a high molecular weight (80−400 kDa) block copolymer alternating linear homopolymeric (poly-α(1−4)-D-galacturonic acid) and branched (poly-α(1−2)-L-rhamnosyl-α(1−4)-D-galacturonosyl with side branches of either α-L-arabinofuranose or α-D-galactopyranose) repeating units [52]. These repeating domains, schematically illustrated in Figure 3, are known as the homogalacturonan (HG) and rhamnogalacturonan-I (RG-I) regions and their relative proportions determine the flexibility and rheological properties of the polymer in aqueous solution: HG regions promote molecular interactions, allowing the formation of hydrogels, while RG regions promote the formation of entangled structures, enhancing the gels' stability [53].

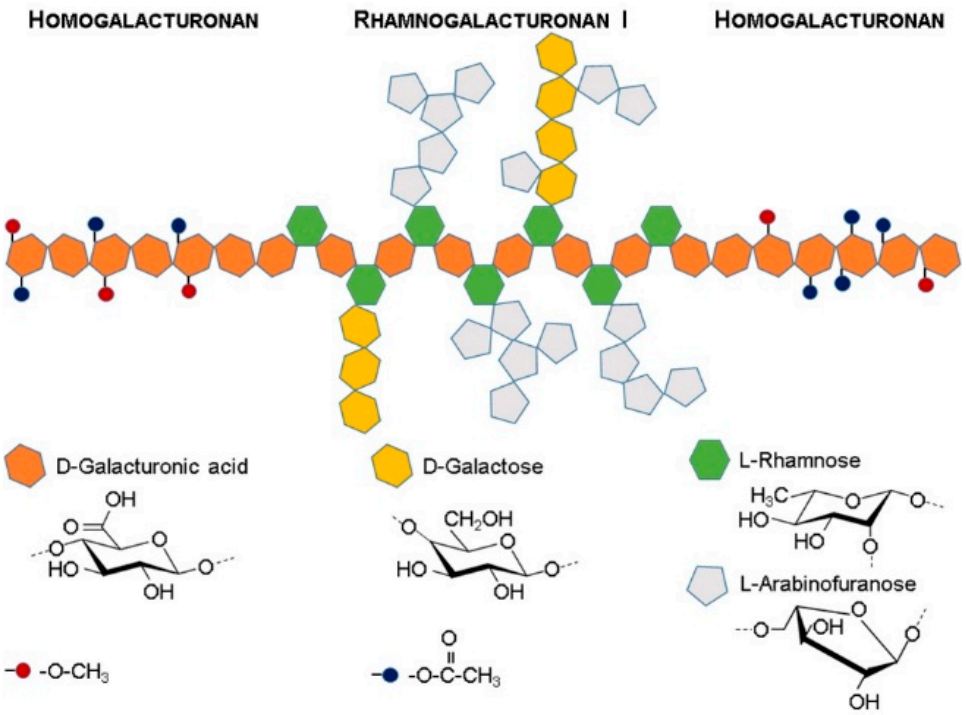

Figure 3. Schematic model of citrus fruits' pectin block copolymer structure, illustrating its two major components: Homogalacturonan and rhamnogalacturonan I.

Some of the homopolymeric galacturonic acid backbone C-2, C-3, and C-5 carboxyl groups may be partially esterified with methoxyl and/or acetyl groups or exist as a uronic acid salt, affecting the polymer charge in solution [54]. The degree of esterification (DE) of pectin (proportion of methoxyl content) determines the gelling mechanism since it influences the availability of COO^- groups in the solution [55]. Typically, pectin with low DE (<50%) tends to promote the presence of charged groups and form gels electrostatically stabilized by metal cations [54], making it particularly appropriate for food, beverage, pharmaceutical, and nutraceutical applications, because it does not require sugar or acidic conditions to gel [56].

Only the aqueous sample labeled as T14 in Figure 2a displaying the WOP1 test, extracted at the end of the process (temperature of 96 °C), was analyzed in quadruplicate. The analysis of the corresponding extracted pectin was carried out 18 months after the test. During this period, the samples of lyophilized pectin, consisting of a pale orange powder with a delicate fragrance, was kept at room temperature in sealed plastic vessels.

The structure of the respective subsamples, labeled as P2, P3, P4, and P5, was characterized by diffuse reflectance infrared Fourier transform (DRIFT) spectroscopy, using a Vertex 70 FTIR spectrometer (Bruker, Ettlingen, Germany) equipped with a wide band mercury cadmium telluride (MCT) detector and a Specac selector, in the 4000 to 500 cm^{-1} range, at 4 cm^{-1} resolution.

The spectra were the result of rationing 500 co-added single beam scans for each sample, i.e., grinded pectin powder (Figure 4) diluted in grinded FTIR grade potassium bromide (KBr) in the appropriate proportion to assure the validity of the Kubelka–Munk assumptions [57], against the same number of scans for the background (grinded KBr). The spectra were converted into Kubelka–Munk units using OPUS^{TM} software (Version 8.2, Bruker Optics, Ettlingen, Germany) and further processed using ORIGIN^{TM} software (Version 8.0, OriginLab Corporation, Northampton, MA, USA).

Figure 4. Sample of lyophilized pectin powder from the WOP1 test (right), which was ground in a quartz mortar (left) prior to the diffuse reflectance infrared Fourier transform (DRIFT) experiments.

2.3.3. Polyphenols Analysis by High Performance Liquid Chromatography with a Diode Array Detector (HPLC-DAD)

After the HC process, the samples collected during the WOP2 test (from T21 to T214) were centrifuged (5 min, 9000 rpm, at 5 °C). The supernatants (5 mL) were then partitioned with n-hexane (5 mL × 3) to completely remove lipophilic compounds, and thus to obtain the aqueous phases. The pellets (process residues) were dried with an oven (40 °C, for 48 h), extracted (5% *w/v*) with 75% ethanol in an ultrasonic bath (30 °C) for 30 min, similarly to the method described in [58], and partitioned with n-hexane (1:1). This extraction method was also applied to dried peels (dry WOP). The extracts were evaporated to dryness, resuspended in methanol and acid water (pH 2.5 by HCOOH) 50:50 (*v/v*), and then injected (15 µL) in a Perkin® Elmer Flexar liquid chromatograph equipped with a quaternary 200Q/410 pump and a LC 200 diode array detector (DAD) (all from Perkin Elmer®, Bradford®, CT, USA).

The stationary phase consisted of an Agilent® Zorbax® SB-18 column (250 × 4.6 mm, 5 µm) kept at 30 °C (Agilent Tech., Palo Alto, CA, USA). The eluents were (A) acidified water (at pH 2.5 adjusted with HCOOH) and (B) acetonitrile/ water (90/10, at pH 2.5 adjusted with HCOOH), and the following gradient was applied: 0–20 min (5–20% B), 20–22 min (20% B), 22–32 min (20–25% B), 32–42 min (25–100% B), and 42–43 min (100–5% B), with an elution flow of 0.6 mL/min.

The quantification of different polyphenols was performed through an external standard method, using stock solutions of the following compounds: Caffeic acid, naringin, and hesperidin (all from Sigma–Aldrich, Milan, Italy). The identification of single compounds was accomplished based on the comparison of their UV-VIS spectra with the literature [58]. All solvents used for the analyses were from Sigma–Aldrich (Milan, Italy). All measurements were performed in triplicate.

2.3.4. Analysis of Terpenes

After the WOP2 test, all the aqueous phase samples (from T21 to T214) and five selected solid residue samples (T21, T22, T26, T210, and T214) were analyzed for terpenes. Moreover, the analyses were also carried out on raw orange peel samples stored at −20 °C.

Liquid extraction was done by mixing 1 mL of aqueous phase samples with the same volume of heptane, containing 20 ppm tridecane as an internal standard [59] in 2 mL glass vials with a Teflon-coated screw cap (Perkin–Elmer, Norwalk, CT, USA).

The solid residue samples were dehydrated on filter paper with a vacuum pump for 5 min, and 0.5 mg (fresh weigh (FW)) of each sample were closed in a glass vial, suspended in 2 mL of heptane with 20 ppm tridecane and a small amount of sodium chloride, and stirred for 5 min at room temperature. This procedure was also applied to raw orange peel samples previously grounded in liquid nitrogen in a mortar to a fine powder (0.5 mg FW).

All samples were incubated in an ultrasonic bath for 30 min at 0 °C and then slowly stirred for 24 h at room temperature. The supernatant (100 µL) was used for analysis after centrifugation at 4000 rpm for 10 min at room temperature in an Eppendorf centrifuge model 5810R (Westbury, NY, USA). The heptane extracts (1 µL) were analyzed using an Agilent 7820A gas chromatograph (GC) interfaced to an Agilent 5977E mass spectrometer (MS) with EI ionization and single quadrupole mass analyzer (Agilent Tech., Palo Alto, CA, USA). A chromatographic column, Agilent HP-INNOWax capillary 50 m length, 0.20 mm radius (ID), 0.4 µm film thickness (DF), was used. The GC injection temperature was 250 °C, splitless mode, and the oven was programmed at 40 °C for 1 min, followed by ramps of 5 °C/min to 200 °C, and 10 °C/min to 260 °C. This high temperature was held for 5 min.

Terpene compounds were identified based on both peaks, matching with the library spectral database (NIST 11) and Kovats retention indices (KRI) retrieved in the literature for the identified compounds. All measurements were performed in triplicate, and the amount of each terpene expressed as a percentage of the total.

3. Results

3.1. Biochemical Methane Generation Potential

Table 2 shows the composition of the solid residues from the samples collected during the WOP1 test, in terms of the relative contents of moisture, ash, volatile substance, carbon, hydrogen, nitrogen, and sulfur, along with the Th-BMP and the theoretical relative content of methane (CH_4) in the biogas. Additionally, the BMP achieved after 36 days is shown.

Table 2. Composition of solid residues from the samples of the WOP1 test. Unless specified otherwise, units are % *w/w* on a dry basis. Theoretical biomethane generation potential (Th-BMP).

Sample	Moisture [1]	Ash	VS	C	H	N	S	Th-BMP [2]	CH_4 [3]	BMP [4]
T11	95.6	3.8	96.2	42.7	6.2	0.7	0.1	421.3	50.0	256
T12	96.6	3.5	96.5	42.2	6.3	0.7	0.1	415.6	49.6	261
T13	97.0	3.2	96.8	42.6	6.2	0.9	0.1	408.9	48.9	318
T14	96.6	2.8	97.2	41.1	6.4	0.7	0.1	392.5	49.3	763

[1] Unit: % *w/w* as determined. [2] Unit: mL/g VS. [3] Unit: % in biogas. [4] After 36 days. Unit: mL/g VS.

Figure 5a shows the cumulated daily biogas generation (in mL) from all the samples, including the blank, resulting from the average of triplicate measurements. At the end of the 36 day period, the biogas generation achieved the levels of 185, 554, 564, 637, and 763 mL for the blank T11, T12, T13, and T14 samples, respectively. The standard deviations of the measurements did not exceed 3% of the average value at the 8th day and afterward (for example, 497 ± 14 mL for the T14 sample at the 8th day), thus visible differences were also statistically significant.

Most of the biogas production from samples T11 to T14 occurred within the first 7–8 days (57% to 68% of the overall generation), while it was delayed and evolved much more linearly with time for the blank sample. In particular, after the first week a substantial part of the biogas generation from samples T11 to T14 was due to emissions from the inoculum (constituting the blank sample).

After the subtraction of the biogas generation from the blank sample and the conversion to methane, based on the relative content of CH_4 in the biogas (as shown in Table 2), the BMP attributed to the solid residues of the samples, extracted during the WOP1 test, could be calculated. Figure 5b shows the assessed cumulated daily methane generation in mL per gram of volatile substance from the samples T11 to T14 during the 36-days biodigestion period.

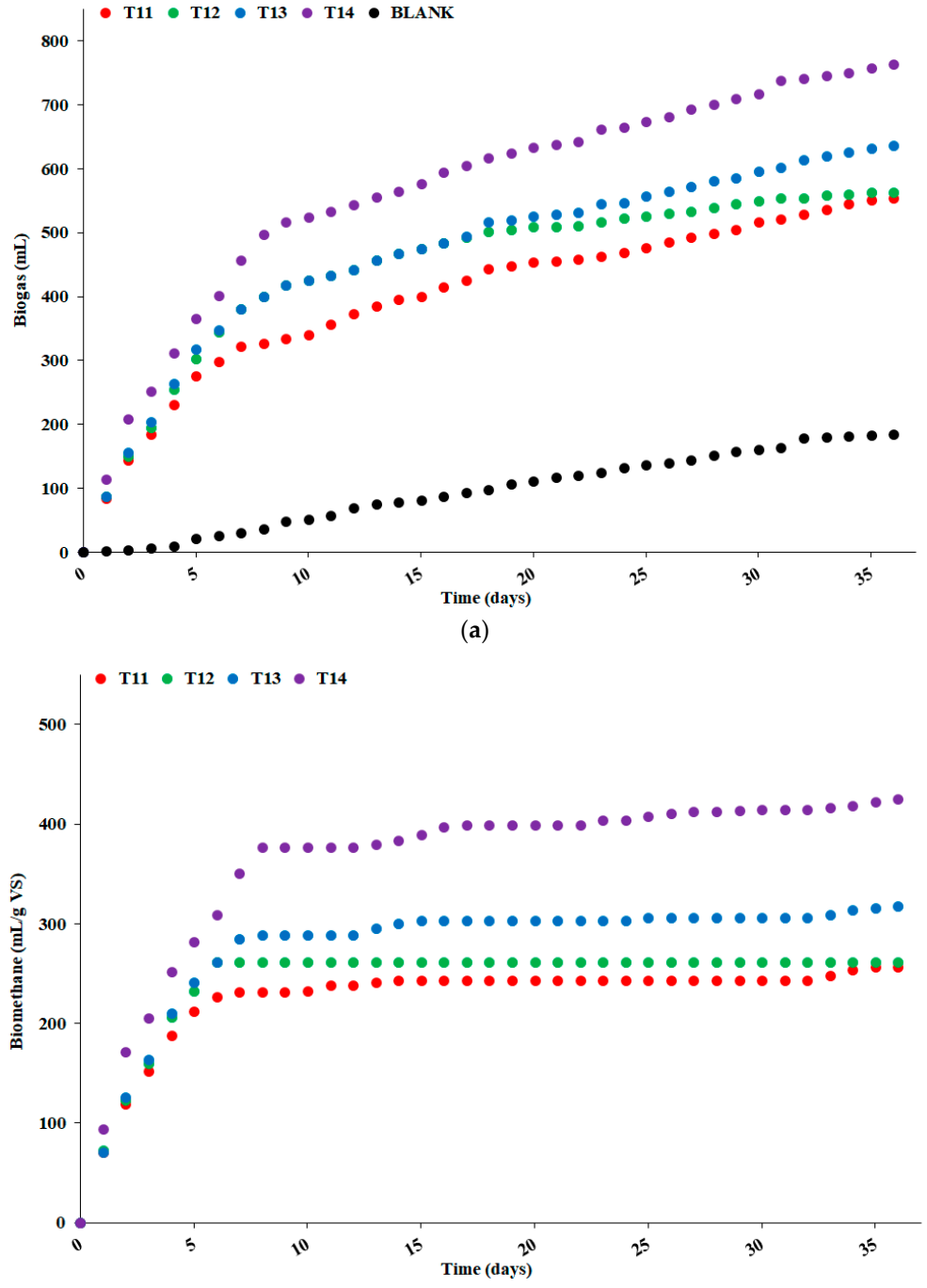

Figure 5. (**a**) Cumulated biogas generation from all the WOP1 test samples, including the blank sample; (**b**) cumulated methane production from all the WOP1 test samples, after subtraction of the generation from the blank sample.

Almost all the methane was generated within the first 7–8 days, varying from 88% for sample T14 to 100% for sample T12. Based on the data shown in Table 2, after 36 days, the actual BMP was −39%, −37%, −22%, and +8% of the Th-BMP for the samples T11, T12, T13, and T14, respectively. Thus, the HC process was able to effectively increase the methane generation from the solid residues of the WOP material, with a clear increasing trend during the hydrocavitation process up to the full exploitation of the respective BMP.

Considering the chemical energy density of the methane at the level of 10.5 kWh/m^3, the data shown in Table 2, and the methane generation rates at the end of the 36-day period mentioned above, Table 3 shows the energy balance of the process for the four analyzed samples. However, electricity and methane chemical energy cannot be directly compared. In particular, the consumed electricity should be converted into the chemical energy of methane needed for power generation, with conversion factors depending on the specific production technology.

Table 3. Energy balance of the process: Consumed specific energy (electricity during the HC process) and specific energy available in the generated methane (chemical energy). Units are kWh/kg fresh weight.

Sample	Consumed Specific Energy	Specific Energy in the Generated Methane
T11	0.01	0.28
T12	0.09	0.28
T13	0.27	0.34
T14	0.62	0.45

3.2. Pectin

Pectin isolated from four subsamples (P2, P3, P4, and P5) by lyophilization of sample T14, collected at the end of the WOP1 test (Figure 2a), was analyzed via DRIFT spectroscopy. Figure 6 shows the corresponding DRIFT spectra (2000–500 cm^{-1} region), which exhibit the typical features of pectin.

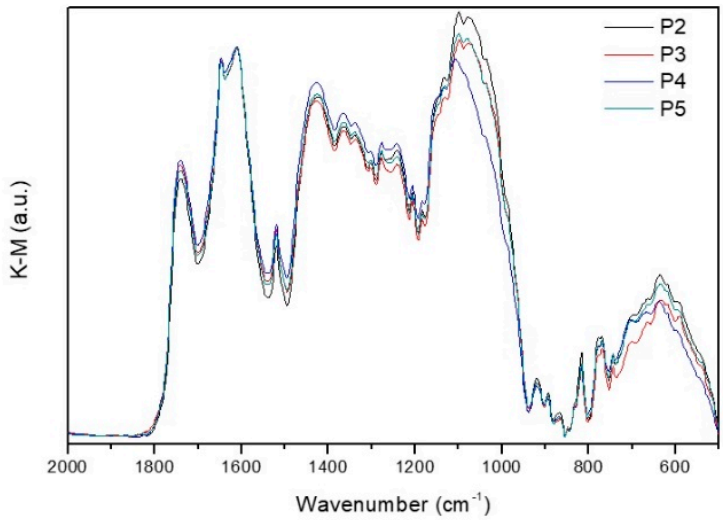

Figure 6. DRIFT spectra of the pectin samples in the 2000–500 cm^{-1} region, normalized to the $\nu_{as}COO^-$ band of carboxylate groups at 1610 cm^{-1}.

The main features in the 1800–1550 cm^{-1} region, with maxima at 1740, 1647, and 1610 cm^{-1}, were assigned to the stretching modes of carbonyl groups from esterified galacturonic acid ($\nu C = O_{ester}$), non-esterified hydrogenated acidic groups ($\nu C = O_{acid}$), and carboxylate groups ($\nu_{as}COO^-$), respectively [13]. The 1550–1200 cm^{-1} region is dominated by CH_x and C-O-H deformation modes, partially overlapped with ester related stretching modes [60,61], and includes:

- The $\delta_{as}CH_3$ and δ_sCH_3 (from ester methyl groups in the galacturonic rings and rhamnose rings of the pectin backbone) at 1520 and 1365 cm^{-1};
- The ν_sCOO^- at 1425 cm^{-1};
- The $\nu C–O–C_{ester}$ at 1277cm^{-1};
- The $\delta_{ip}C–O–H$ (from alcohol hydroxyl groups in the pyranose rings of the pectin chain) at 1242 cm^{-1}.

The 1200–950 cm^{-1} region includes a set of very intense bands partially overlapped, typical of pectin, assigned to skeletal (νC–C), C–O–C stretching (νC–O–C) modes of the pyranose rings and glycosidic bonds, and to a combination of the νC–OH and νC–C modes from the pyranose rings [62,63]. Finally, the 950–500 cm^{-1} region contains the bands related to the external deformation vibrations of methyl, methylene, and methyne groups (ρCH_x and δC–H) [61].

The degree of esterification of pectin (percent of esterified carboxyl groups) was determined by spectral analysis of the 1800–1550 cm^{-1} region, such as the ratio of ester carboxyl to total carboxyl peak areas, as shown in Equation (3) [64]:

$$DE = \Sigma A_{\nu C=Oester} / (\Sigma A_{\nu C=Oester} + A_{\nu C=Oacid} + A_{\nu asCOO^-}) \quad (3)$$

The νC = O and $\nu_{as}COO^-$ band areas were estimated by decomposing the 1900–850 cm^{-1} region (two consecutive absorption zeros) into a sum of Gaussian components, using a nonlinear least-squares fitting [13].

Table 4 summarizes the components' centers, full width at half maxima, and integrated areas obtained for the four samples. Based on these results, it was possible to determine a rather low degree of esterification for this pectin, namely 17.05 ± 0.60%.

Table 4. Decomposition results of the 1800–1550 cm^{-1} region of the DRIFT spectra: Centers (C), full width at half maxima (FWHM), integrated areas (A) of the νC = O and $\nu_{as}COO^-$ band areas, and degree of esterification (DE).

Sample	Band Areas	C (cm^{-1})	FWHM (cm^{-1})	A(a.u.)	DE
P2	$\nu C=O_{ester}$	1741	47	28.03	0.1786
	$\nu C=O_{acid}$	1648	18	3.37	
	$\nu_{as}COO^-$	1608	137	125.50	
P3	$\nu C=O_{ester}$	1740	50	28.67	0.1715
	$\nu C=O_{acid}$	1649	19	3.04	
	$\nu_{as}COO^-$	1609	143	135.42	
P4	$\nu C=O_{ester}$	1741	48	28.66	0.1664
	$\nu C=O_{acid}$	1648	18	3.05	
	$\nu_{as}COO^-$	1610	148	140.55	
P5	$\nu C=O_{ester}$	1741	47	28.55	0.1655
	$\nu C=O_{acid}$	1648	19	3.09	
	$\nu_{as}COO^-$	1610	149	140.87	

3.3. Polyphenols

As an example, Figure 7 shows the chromatograms of the sample T28 (39 min, 40.5 °C), its pellet (process residues), and the dry WOP. As expected, the flavanones naringin and hesperidin dominated the chromatogram of the dry WOP, along with another peak, labeled as F5 and classified as an unidentified flavanone derivative, according to its UV spectra. The same features dominated the chromatogram of the pellet, although with a lower relative contribution of naringin.

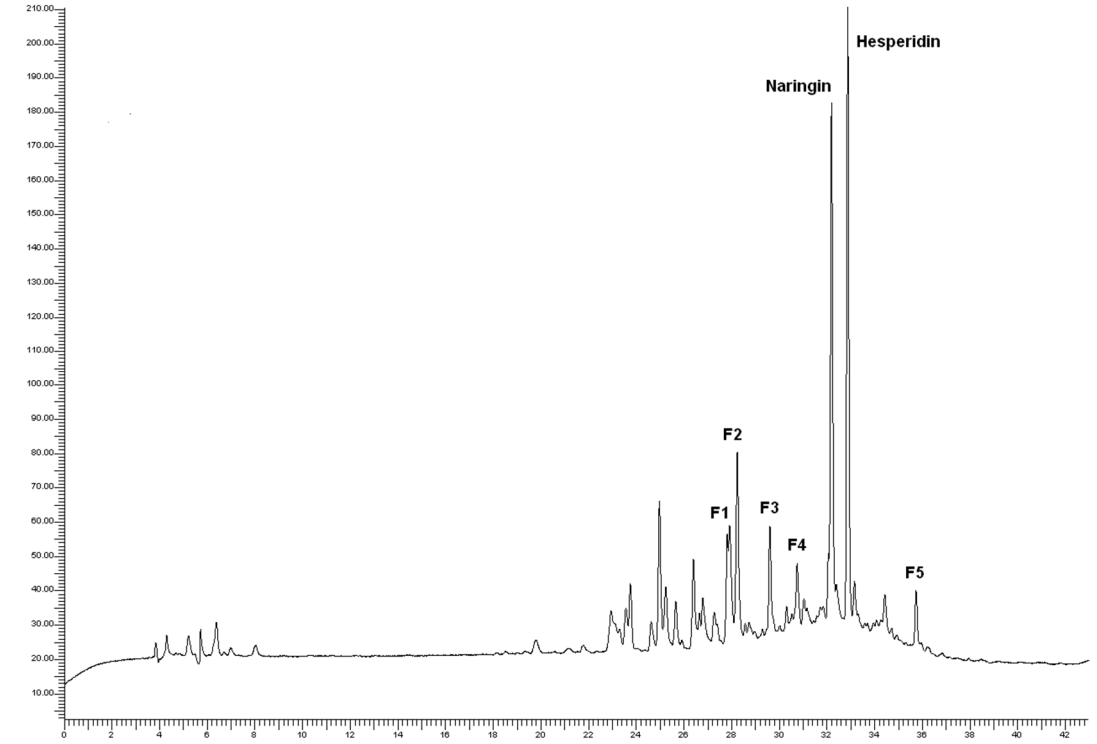

(**a**)

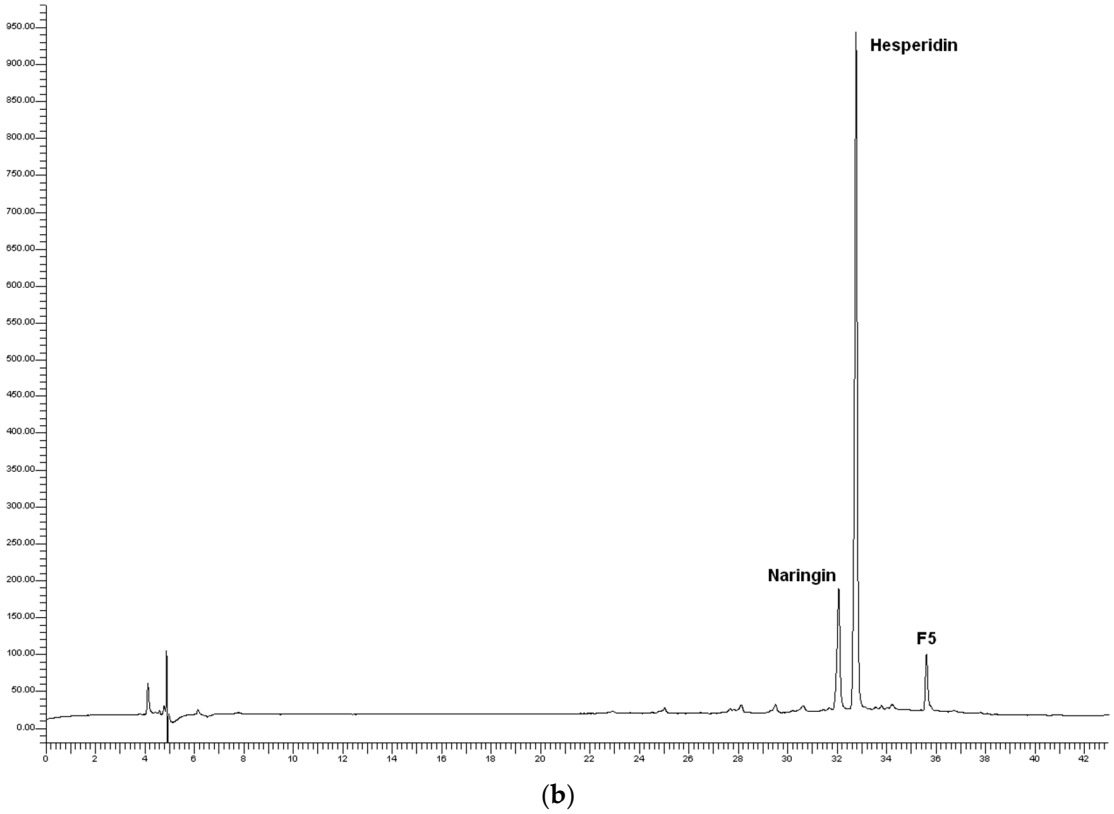

(**b**)

Figure 7. *Cont.*

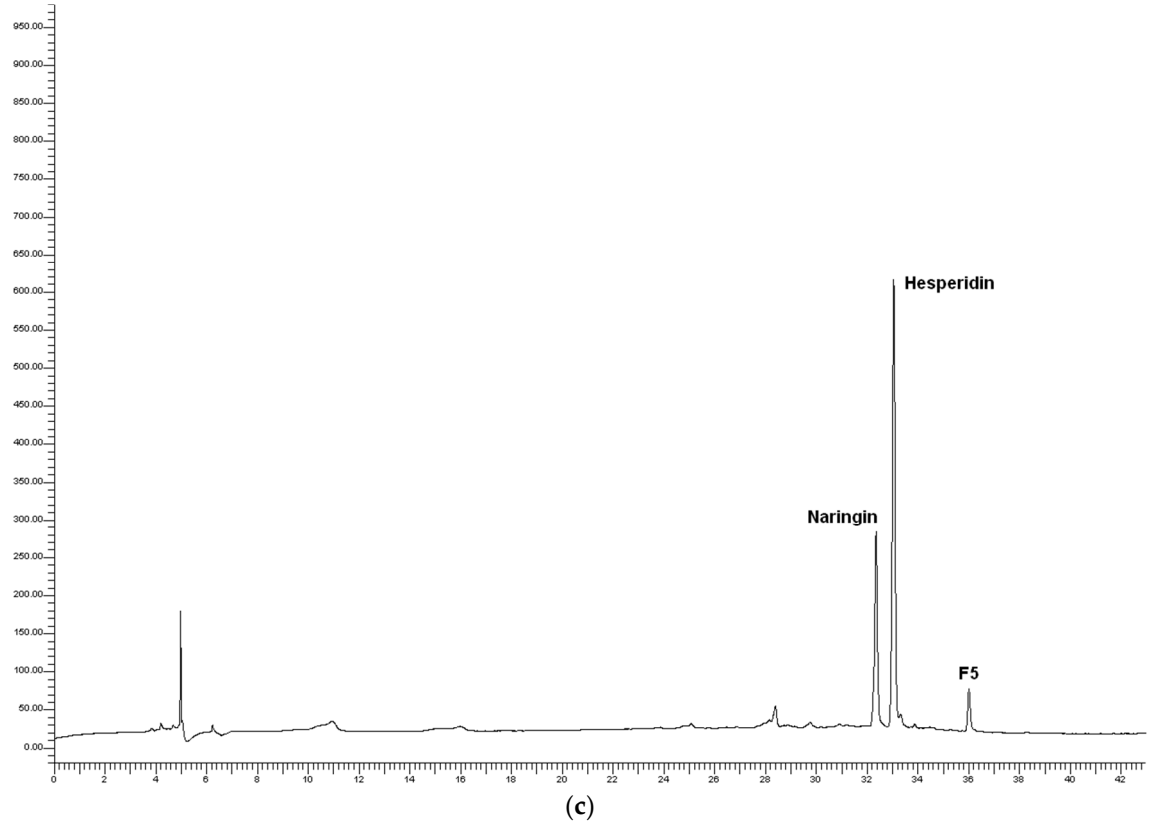

Figure 7. Chromatograms of polyphenols for the sample T28 of the test WOP2: (**a**) Aqueous phase; (**b**) process residues; (**c**) dry WOP.

In the aqueous phase, along with the peaks attributed to naringin and hesperidin, the peaks labeled as F1 to F4 were detected and identified as flavanone derivatives based on their UV spectra. The unlabeled peaks were putatively identified as hydroxycinnamic acid derivatives (HAD), based on their UV spectra similar to those of caffeic acid, with absorbance peak around 330 nm, instead of 280 nm, as for flavanones [65].

Figure 8 shows the total polyphenolic content (flavanones and HAD) present in the aqueous phase of the whole system (total volume = 147 L). Sample T27 (30 min, 37 °C) exhibited a total polyphenols content significantly lower than all the samples from T22 to T214 ($p < 0.05$). Moreover, the total polyphenolic content of the sample T23 was significantly higher than that of sample T28 ($p < 0.05$).

Quite surprisingly, the higher content of polyphenols, mostly due to the increase of naringin and other flavanones (F1–F5), was reached after 10 min from the beginning of the process time (sample T23, temperature of 24 °C), corresponding to about 30 passes of the entire volume of the processed mixture through the cavitation reactor. Moreover, the apparent stability of the total content up to the sample T26 (20 min, 30 °C), and the following rather abrupt decrease at T27 (30 min, 35 °C), in turn followed by the return to the levels typical of T23–T26, could suggest a possible kinetics involving thermal degradation and further extraction from the circulating WOP.

The total contents of naringin, hesperidin, and other flavanones (F1–F5) in the raw fresh WOP (6.379 kg) were 16.39, 36.26, and 2.95 g, respectively. Based on these data, and the total contents (including HAD) observed in the aqueous phase (Figure 8), the extraction yields peaked in correspondence of the samples T23 (59.5%) and T24 (59.6%). However, the extraction yield was already as high as 53.5% at T21, i.e., after just 2 min of process time and about 6 passes of the entire volume of the processed mixture through the cavitation reactor.

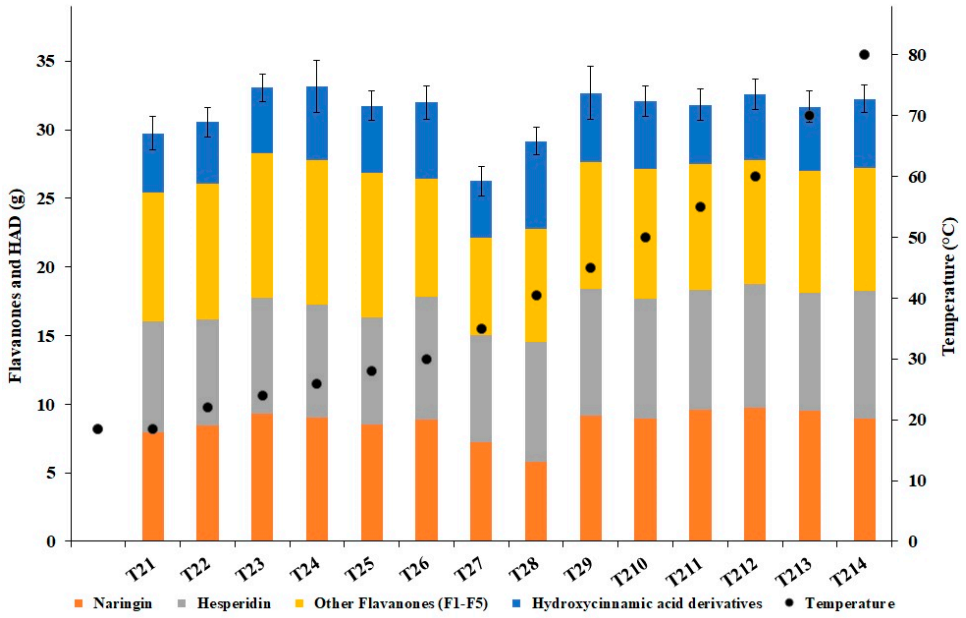

Figure 8. Content of flavanones and hydroxycinnamic acid derivatives in the aqueous phase.

3.4. Terpenes

Figure 9 shows the concentration of the detected monoterpenes in the aqueous phase and the solid residues, derived from the observed concentration in each of the samples collected during the WOP2 test. In the aqueous phase (Figure 9a, unit ng/mL), *d*-limonene represented more than 73% of all monoterpenes in any of the first seven samples and, in particular, more than 93% in sample T22. In the solid residues (Figure 9b, in ng/g fresh weight, except for *d*-limonene, expressed in µg/g fresh weight), *d*-limonene represented more than 96% of all monoterpenes in any sample.

The concentration of *d*-limonene in the aqueous solution more than doubled from the sample T21 (2 min, 18.5 °C) to T22 (6 min, 22 °C); such a pattern was shared by the other detected monoterpenes, although with milder changes. As mentioned in Section 2.2, volatile compounds were free to escape from the processing device, which explains why the limonene concentration decreased abruptly by almost 80% from the sample T22 to T23 (10 min, 24 °C). The *d*-limonene content stabilized around similar levels, eventually further decreasing from sample T28 (39 min, 40.5 °C) onwards, reaching zero in the last sample T214 (127 min, 80 °C), along with all the other terpenes. Beyond cavitation, temperature appears to play an essential role in the volatilization of the terpenes.

The fast and effective extraction of *d*-limonene from the WOP was confirmed by the abrupt decrease of its concentration (by about 45%) in the solid residues, from sample T21 to sample T22, again stabilizing around similar levels onwards. Noticeably, the mass of solid residues decreased substantially during the HC-based process (as visually observed). Hence, the respective actual content of *d*-limonene probably decreased much more than represented in Figure 9b.

In the raw WOP, limonene accounted for over 96% of all monoterpenes, with a concentration of 5.9 ± 0.9 µg/g FW. Based on the original WOP mass (fresh weight) of 6.379 kg, a total content of 38 ± 6 mg of *d*-limonene in the raw material was estimated. The peak concentration in the aqueous phase (sample T22) was 18.7 ± 0.5 ng/mL, which, multiplied by the volume of the water (147 L), translates into a total content of 2.75 ± 0.07 mg, i.e., a yield just over 7%. However, it is unknown how much terpene escaped the hydrocavitation open reactor during the first 6 min of the process, and data concerning the solid residues suggest that the actual extraction yield was substantially higher, at least up to 45%.

Finally, it is interesting to notice that, among the other detected monoterpenes, myrcene was the most relatively abundant in the solid residues, while linalool prevailed in the aqueous solution, in full agreement with the alcohol nature of the latter.

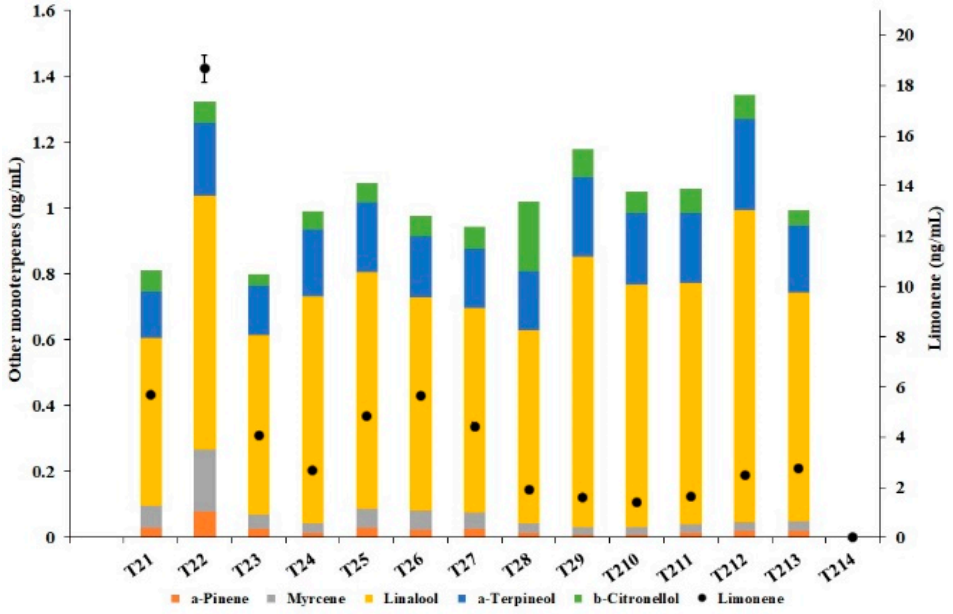

(**a**)

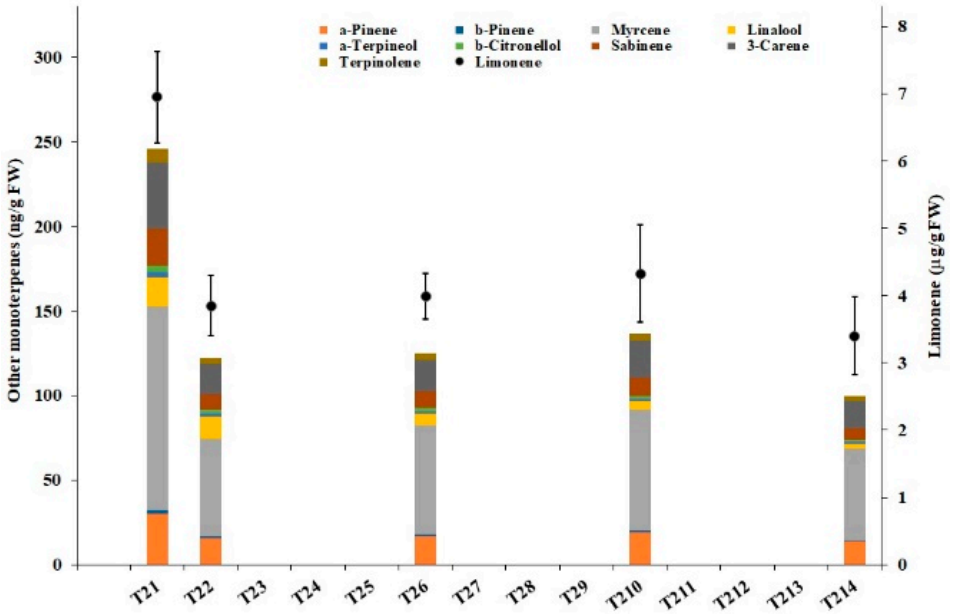

(**b**)

Figure 9. Concentration of monoterpenes: (**a**) Aqueous phase; (**b**) solid residues.

4. Discussion

The device used to process the orange peel waste, employing no proprietary components, is easy to construct and maintain, and its operation, at the pre-industrial scale, was verified by experiments carried out on real scale (more than 100 L of water, quantity of WOP raw material of about 6.4 and 42 kg). The scalability of the proposed device, up to the industrial scale (1700 L), was recently demonstrated in the brewing sector [66]. Additionally, the reliability of the device was proven by the absence of any wear of flow components after thousands of hours of operation, as was already noted in a previous study using the device [30].

The hydrodynamic cavitation processes, sustained by a circular Venturi-shaped reactor, allowed us to effectively and completely separate and extract the most valued components of the waste orange peel. It is remarkable that no solvents or any additives, other than tap water, were used in the extraction processes.

As shown in Section 3.1, the biomethane generation potential was boosted in terms of both total cumulated production and generation rate. Within only 3 min at 14.5 °C, corresponding to less than 10 passes of the entire processed mixture through the cavitation reactor, the BMP was already at 61% of its theoretical value. Additionally, the specific energy content of the generated methane (chemical energy) was about 30 times higher than the specific consumed energy (electricity). Since then, the BMP increased up to the Th-BMP at the end of the process WOP1 (273 min, temperature of 96 °C), but the energy balance became negative.

From the energy balance point of view, it would be imperative to limit the processing time as much as possible, i.e., to a few min. However, the processing time should be optimized based on the assessment of the overall value of the extractable materials, such as pectin, polyphenols, and terpenes, as well as on the processing of the substrate resulting from the anaerobic digestion (e.g., disposal, composting). Such topics will require further research.

Due to the apparent suboptimal cavitation regime during most of the WOP1 process, especially during the first 60–90 min, it is likely that simple technical adjustments, such as a different centrifugal pump, could produce even better results. However, with a lower concentration of WOP in the aqueous mixture, as in the WOP2 test, the HC process was carried out in the optimal regime, as proven by the low levels of the cavitation number. Thus, an optimized HC process is expected to lead to higher methane generation in a shorter process time, even for higher WOP concentrations, thereby further improving the energy balance.

According to the results presented in Section 3.2, the pectin isolated in the sample collected at the end of the WOP1 process showed a very low degree of esterification, namely 17.05 ± 0.60%, meaning that it would be particularly appropriate for food and beverage, pharmaceutical, and nutraceutical applications, because it does not require sugar or acidic conditions to form stabilized gels. It should be noted that this result nicely agrees with previous studies, in which pectin from WOP originating from red oranges from the same area of Sicily, extracted via microwave hydrodistillation and gravity, was shown to have a DE of 25%, suggesting that the pectin from the red orange pulp is likely to have a very low DE [67]. However, a distinct beneficial role of the HC-based extraction method on the pectin DE cannot be ruled out, which deserves further comparative research.

We remind that WOP (exo-, meso-, and endocarp) contains not only the outer skin (exocarp) and the peel (exo- and mesocarp), but also endocarp residues. It is remarkable that, as mentioned in Section 2.3.2., pectin, analyzed 18 months after extraction and lyophilization, remained stable during prolonged storage at room temperature in direct contact with oxygen. In fact, after another three months in the same plastic vessel, pectin continued to show no sign of degradation. This evidence pointed to the stabilization effect of powerful antioxidant orange biophenols, including the flavanones (Section 3.3) found in the WOP2 aqueous solutions, and is likely available in an even higher concentration in the sample T14 from the WOP1 test.

Overall, the WOP1 test proved that the HC process allowed the effective extraction of high-quality pectin from the waste orange peel and a very efficient exploitation of the biomethane generation potential from the solid residues of the process. Additionally, there was no evidence of microbiological degradation or spoilage in the T14 liquid sample, even though it was unlikely that any relevant concentration of antimicrobial *d*-limonene remained in the aqueous solution, due to the very high working temperature (as shown for sample T214 from the WOP2 test). We hypothesize that the reason for the apparent microbiological stability lies in the well-known effective disinfection carried out by the HC-thermal process [40]. The stabilization effects produced by the extracted flavanones and the process-driven disinfection could be distinctive features of the HC-based extraction method.

As shown in Section 3.3, water-soluble flavanones, naringin and hesperidin, constituted the majority of polyphenols in the WOP. Both compounds were extracted in the aqueous solution quite effectively and efficiently through the HC process and were partially transformed into other compounds, mostly other flavanones and possibly hydroxycinnamic acid derivatives. Overall, the extraction process yield was nearly 60%, regarding the sum of the detected compounds. Such a level was achieved within 10 min of processing, while after just 2 min it was at about 53%, thus proving the effectiveness of the extraction.

The HC-based polyphenols extraction rate was remarkably greater than achieved by means of a state-of-the-art hydro-distillation extraction method [17], where the total polyphenol content in the aqueous phase was only about 17% of the original content, as well as the HC-based extraction was much faster.

We hypothesize that the other flavanones (peaks F1 to F4 in Figure 7) might have derived from hesperidin and/or naringin, following the loss of at least one hexose unit. In their turn, since these peaks were practically undetectable in the chromatogram of the process residues, this decomposition could have been due to cavitation processes occurring in the liquid phase. In addition, the peaks shown just on the left of the peak F1 region in the chromatogram for the aqueous phase (Figure 7, unlabeled peaks), attributed to HAD, were not observed in dry WOP or process residues and could be considered as a distinct effect of the cavitation process.

From the decrease of *d*-limonene concentration in the solid residues (Section 3.4), a lower limit of 45% for the respective extraction yield in the aqueous phase was inferred, such a compound being by far the most abundant monoterpene in the WOP. However, the actual extraction yield is expected to be much higher, as suggested by two pieces of evidence. First, the abrupt drop of its concentration in the aqueous phase shortly after its highest value (6 min of process time) is achieved, pointing to its fast volatilization. Second, the mass loss from the solid residues due to the continuous extraction leads to the overestimation of the respective total content of *d*-limonene, based on its concentration. In forthcoming practical applications, airtight HC extractors will be used in order to retain liquid limonene, both floating and emulsified in the aqueous solution due to the emulsifying action of pectin [15].

While postponing the comparison of EO extraction rates to future experiments, based on the available data it can be safely stated that the HC-based EO extraction was remarkably faster than achieved by means of a state-of-the-art hydro-distillation extraction method [17], which took about 120 min to complete. The same holds with regard to an innovative solvent-free process based on microwave distillation, hydrodiffusion, and gravity [13], where the semi-industrial process took about 60 min.

The high volatility of orange peel EOs under environmental conditions (in particular *d*-limonene, which is chemically unstable) hinders their effectivity as flavorings in the food industry (affecting the shelf-life) and as biopesticides in agronomic applications [68]. Moreover, the antimicrobial action of *d*-limonene was found to markedly increase when applied as an oil-in-water nanoemulsion, for example reducing the thermal resistance of *Listeria monocytogenes* by 100 times, against only two to five times when added directly [69].

Therefore, methods have been proposed to reduce the volatility, increase the stability, and control the release of such compounds. Two recent studies suggested the nanoencapsulation of orange peel EOs [70] and *d*-limonene [71], respectively, in oil-in-water nanoemulsions prepared by ultrasonic irradiation (acoustic cavitation) and stabilized with a mixture of pectin and whey proteins. Thus, the combination of cavitation processes and pectin appears very promising for the retention and effectivity of *d*-limonene, provided its early volatilization is prevented.

Indeed, the residual retention of *d*-limonene in the aqueous solution, up to sample T27 (30 min, 35 °C) in the WOP2 test (Figure 9a), could have been favored by two factors. First, the likely micronization and partial emulsification of the terpenes in water, based on the well-established effectivity of HC processes in the creation of stable sub-micron oil-in-water emulsions [41,72]. Second, the effectivity of pectin as an emulsifying compound, as well as a stabilizer for emulsions [15]. Due to the effective extraction of high-quality pectin in the aqueous phase (Section 3.2), the micronized

limonene drops could have been partly emulsified and stabilized, concurring to the limitation of its volatilization. Future research will investigate these relevant emulsion chemistry aspects.

Further research using optimized devices and processes will allow more comprehensive and rigorous comparison of the presented process with either conventional or newer extraction techniques. As an example, the effective retaining and recovery of orange peel oil during the HC process will allow the determination of comprehensive performance indices, such as those recently advanced, based on the extraction yield, energy efficiency, and quality of the product [73].

Finally, hydrodynamic cavitation techniques were compared many times with competing techniques, very often resulting in higher process yields [33]. Nevertheless, separating and quantifying the contribution of cavitation to the achieved results, in comparison with other processes, such as pumping, heating, and turbulence, would be desirable. Although prevented in this study due to technical limitations, this issue could be solved by means of the installation of a bypass excluding the cavitation reactor, all else being equal, which is recommended for further research. Additionally, the direct visualization of cavitation could be useful in order to assess its features (extent, intensity), which could be done by means of reactors made of transparent material.

5. Conclusions

This study reports remarkable results concerning the valorization of waste orange peel via controlled hydrodynamic cavitation. One of its strengths is the presentation of results obtained on a semi-industrial scale, namely the extraction from 42 kg of WOP with 120 L of tap water (test WOP1). This allowed us to prove the scalability of the process, which is often an issue in laboratory studies dealing with the extraction of valued bioproducts from (at most) a few hundred grams of a biological matrix.

Although the extraction conditions were far from optimal under various aspects, both water-soluble flavanones and *d*-limonene (by far the most abundant monoterpene in red orange and Washington Navel orange EO) were extracted within 10 min of process time and at room temperature. High-quality (low degree of esterification and high molecular weight) pectin was isolated from the aqueous extract via straightforward lyophilization. The cellulose- and hemicellulose-rich solid residue revealed excellent methane generation potential under anaerobic digestion, with a few minutes of process time being sufficient to result in a high ratio of the energy contained in the generated methane to the consumed energy.

The results presented in this study open the route to the integral valorization of WOP via a simple, low cost, and highly effective technology, requiring water as the unique additional raw material. The relevance of these findings also arises from the abundance of WOP (around 25 MT/year as a by-product of the agrifood industry), the anticipated applicability to the processing by-products of other citrus fruits, and the rapid spreading of the controlled HC processes in several food-related products [25,26,32].

The process applied in this study adheres to the six principles of green extraction [74], even though wide margins for further improvement, based on thorough optimization, clearly exist.

Author Contributions: Conceptualization, F.M., C.B., L.A., F.Z., and M.P.; data curation, F.M., C.B., A.F., R.C., L.A., A.G., L.B.d.S.N., and A.D.C.; formal analysis, F.M. and M.P.; funding acquisition, F.M., R.D., F.F., and M.P.; investigation, F.M., C.B., R.C., R.D., L.A., A.D.C., and M.P.; methodology, F.M., C.B., A.F., R.C., R.D., L.A., A.G., L.B.d.S.N., A.D.C., and L.M.I.; resources, F.M., R.D., and M.P.; software, C.B., A.F., A.G., L.B.d.S.N., and A.D.C.; supervision, F.M., F.F., and M.P.; validation, F.M., C.B., A.D.C., and L.M.I.; visualization, F.M, C.B., A.F., A.G., and A.D.C.; writing—original draft, F.M. and F.Z.; writing—review and editing, F.M., C.B., A.F., F.Z., F.F., L.M.I., and M.P.

Funding: This research received no external funding.

Acknowledgments: The authors gratefully acknowledge Dr. Mauro Centritto (CNR-IPSP) for the continuous support and very important suggestions. Special thanks to Mr. Gabriele Cencetti (CNR-IBBR and Laboratory for the Analysis and Research in Environmental Chemistry-ARCA, CNR) for the technical assistance with GC–MS analyses.

Conflicts of Interest: The authors declare no conflict of interest.

References

1. Satari, B.; Karimi, K. Citrus processing wastes: Environmental impacts, recent advances, and future perspectives in total valorization. *Resour. Conserv. Recycl.* **2018**, *129*, 153–167. [CrossRef]
2. USDA—United States Department of Agriculture. Foreign Agricultural Service. Citrus: World Markets and Trade. 2019; pp. 1–11. Available online: https://apps.fas.usda.gov/psdonline/circulars/citrus.pdf (accessed on 25 July 2019).
3. Negro, V.; Ruggeri, B.; Fino, D.; Tonini, D. Life cycle assessment of orange peel waste management. *Resour. Conserv. Recycl.* **2017**, *127*, 148–158. [CrossRef]
4. Ciriminna, R.; Fidalgo, A.; Delisi, R.; Carnaroglio, D.; Grillo, G.; Cravotto, G.; Tamburino, A.; Ilharco, L.M.; Pagliaro, M. High-Quality essential oils extracted by an eco-friendly process from different citrus fruits and fruit regions. *ACS Sustain. Chem. Eng.* **2017**, *5*, 5578–5587. [CrossRef]
5. Pourbafrani, M.; Forgács, G.; Horváth, I.S.; Niklasson, C.; Taherzadeh, M.J. Production of biofuels, limonene and pectin from citrus wastes. *Bioresour. Technol.* **2010**, *101*, 4246–4250. [CrossRef] [PubMed]
6. Ciriminna, R.; Lomeli-Rodriguez, M.; Demma Carà, P.; Lopez-Sanchez, J.A.; Pagliaro, M. Limonene: A versatile chemical of the bioeconomy. *Chem. Commun.* **2014**, *50*, 15288–15296. [CrossRef] [PubMed]
7. Singh, G.; Upadhyay, R.K.; Narayanan, C.S.; Padmkumari, K.P.; Rao, G.P. Chemical and fungitoxic investigations on the essential oil of Citrus sinensis (L.) Pers. *J. Plant Dis. Prot.* **1993**, *100*, 69–74.
8. Hollingsworth, R.G. Limonene, a citrus extract, for control of mealybugs and scale insects. *J. Econ. Entomol.* **2005**, *98*, 772–779. [CrossRef] [PubMed]
9. Keinan, E.; Alt, A.; Amir, G.; Bentur, L.; Bibi, H.; Shoseyov, D. Natural ozone scavenger prevents asthma in sensitized rats. *Bioorganic Med. Chem.* **2005**, *13*, 557–562. [CrossRef] [PubMed]
10. Fitzgerald, C.; Hossain, M.; Rai, D.K. Waste/By-Product Utilisations. In *Innovative Technologies in Beverage Processing*; Aguiló-Aguayoi, I., Plaza, L., Eds.; John Wiley & Sons, Ltd.: Chichester, UK, 2017; pp. 297–309.
11. Pagliaro, M.; Rosaria, C.; Fidalgo, A.M.A.; Delisi, R.; Ilharco, L. Pectin production and global market. *Agro Food Ind. Hi Tech* **2016**, *27*, 17–20.
12. Ciriminna, R.; Chavarría-Hernández, N.; Inés Rodríguez Hernández, A.; Pagliaro, M. Pectin: A new perspective from the biorefinery standpoint. *Biofuels Bioprod. Biorefining* **2015**, *9*, 368–377. [CrossRef]
13. Fidalgo, A.; Ciriminna, R.; Carnaroglio, D.; Tamburino, A.; Cravotto, G.; Grillo, G.; Ilharco, L.M.; Pagliaro, M. Eco-Friendly extraction of pectin and essential oils from orange and lemon peels. *ACS Sustain. Chem. Eng.* **2016**, *4*, 2243–2251. [CrossRef]
14. Leroux, J.; Langendorff, V.; Schick, G.; Vaishnav, V.; Mazoyer, J. Emulsion stabilizing properties of pectin. *Food Hydrocoll.* **2003**, *17*, 455–462. [CrossRef]
15. Dickinson, E. Hydrocolloids acting as emulsifying agents—How do they do it? *Food Hydrocoll.* **2018**, *78*, 2–14. [CrossRef]
16. Boukroufa, M.; Boutekedjiret, C.; Petigny, L.; Rakotomanomana, N.; Chemat, F. Bio-refinery of orange peels waste: A new concept based on integrated green and solvent free extraction processes using ultrasound and microwave techniques to obtain essential oil, polyphenols and pectin. *Ultrason. Sonochem.* **2015**, *24*, 72–79. [CrossRef] [PubMed]
17. Hilali, S.; Fabiano-Tixier, A.S.; Ruiz, K.; Hejjaj, A.; Ait Nouh, F.; Idlimam, A.; Bily, A.; Mandi, L.; Chemat, F. Green extraction of essential oils, polyphenols, and pectins from orange peel employing solar energy: Toward a zero-waste biorefinery. *ACS Sustain. Chem. Eng.* **2019**, *7*, 11815–11822. [CrossRef]
18. Holkar, C.R.; Jadhav, A.J.; Pinjari, D.V.; Pandit, A.B. Cavitationally driven transformations: A technique of process intensification. *Ind. Eng. Chem. Res.* **2019**, *58*, 5797–5819. [CrossRef]
19. Gogate, P.R.; Pandit, A.B. Hydrodynamic cavitation reactors: A state of the art review. *Rev. Chem. Eng.* **2001**, *17*, 1–85. [CrossRef]
20. Pawar, S.K.; Mahulkar, A.V.; Pandit, A.B.; Roy, K.; Moholkar, V.S. Sonochemical effect induced by hydrodynamic cavitation: Comparison of venturi/orifice flow geometries. *AIChE J.* **2017**, *63*, 4705–4716. [CrossRef]
21. Yasui, K.; Tuziuti, T.; Sivakumar, M.; Iida, Y. Sonoluminescence. *Appl. Spectrosc. Rev.* **2004**, *39*, 399–436. [CrossRef]
22. Dindar, E. An overview of the application of hydrodinamic cavitation for the intensification of wastewater treatment applications: A review. *Innov. Energy Res.* **2016**, *5*, 1–7. [CrossRef]

23. Doltade, S.B.; Dastane, G.G.; Jadhav, N.L.; Pandit, A.B.; Pinjari, D.V.; Somkuwar, N.; Paswan, R. Hydrodynamic cavitation as an imperative technology for the treatment of petroleum refinery effluent. *J. Water Process Eng.* **2019**, *29*, 100768. [CrossRef]
24. Ciriminna, R.; Albanese, L.; Meneguzzo, F.; Pagliaro, M. Wastewater remediation via controlled hydrocavitation. *Environ. Rev.* **2017**, *25*, 175–183. [CrossRef]
25. Carpenter, J.; Badve, M.; Rajoriya, S.; George, S.; Saharan, V.K.; Pandit, A.B. Hydrodynamic cavitation: An emerging technology for the intensification of various chemical and physical processes in a chemical process industry. *Rev. Chem. Eng.* **2017**, *33*, 433–468. [CrossRef]
26. Panda, D.; Manickam, S. Cavitation technology—The future of greener extraction method: A review on the extraction of natural products and process intensification mechanism and perspectives. *Appl. Sci.* **2019**, *9*, 766. [CrossRef]
27. Cravotto, G.; Mariatti, F.; Gunjevic, V.; Secondo, M.; Villa, M.; Parolin, J.; Cavaglià, G. Pilot scale cavitational reactors and other enabling technologies to design the industrial recovery of polyphenols from agro-food by-products, a technical and economical overview. *Foods* **2018**, *7*, 130. [CrossRef] [PubMed]
28. Sarvothaman, V.P.; Simpson, A.T.; Ranade, V.V. Modelling of vortex based hydrodynamic cavitation reactors. *Chem. Eng. J.* **2018**. [CrossRef]
29. Asaithambi, N.; Singha, P.; Dwivedi, M.; Singh, S.K. Hydrodynamic cavitation and its application in food and beverage industry: A review. *J. Food Process Eng.* **2019**, e13144. [CrossRef]
30. Albanese, L.; Ciriminna, R.; Meneguzzo, F.; Pagliaro, M. Beer-brewing powered by controlled hydrodynamic cavitation: Theory and real-scale experiments. *J. Clean. Prod.* **2017**, *142*, 1457–1470. [CrossRef]
31. Albanese, L.; Ciriminna, R.; Meneguzzo, F.; Pagliaro, M. Innovative beer-brewing of typical, old and healthy wheat varieties to boost their spreading. *J. Clean. Prod.* **2018**, *171*, 297–311. [CrossRef]
32. Albanese, L.; Bonetti, A.; D'Acqui, L.P.; Meneguzzo, F.; Zabini, F. Affordable production of antioxidant aqueous solutions by hydrodynamic cavitation processing of silver fir (Abies Alba Mill.) needles. *Foods* **2019**, *8*, 65. [CrossRef]
33. Albanese, L.; Meneguzzo, F. 10—Hydrodynamic cavitation technologies: A pathway to more sustainable, healthier beverages, and food supply chains. In *Processing and Sustainability of Beverages*; Grumezescu, A.M., Holban, A.M., Eds.; Woodhead Publishing: Sawston, Cambridge, UK, 2019; pp. 319–372. ISBN 978-0-12-815259-1.
34. Fernandez, M.E.; Ledesma, B.; Román, S.; Bonelli, P.R.; Cukierman, A.L. Development and characterization of activated hydrochars from orange peels as potential adsorbents for emerging organic contaminants. *Bioresour. Technol.* **2015**, *183*, 221–228. [CrossRef] [PubMed]
35. Lam, S.S.; Liew, R.K.; Lim, X.Y.; Ani, F.N.; Jusoh, A. Fruit waste as feedstock for recovery by pyrolysis technique. *Int. Biodeterior. Biodegrad.* **2016**, *113*, 325–333. [CrossRef]
36. Ciriminna, R.; Albanese, L.; Di Stefano, V.; Delisi, R.; Avellone, G.; Meneguzzo, F.; Pagliaro, M. Beer produced via hydrodynamic cavitation retains higher amounts of xanthohumol and other hops prenylflavonoids. *LWT Food Sci. Technol.* **2018**, *91*, 160–167. [CrossRef]
37. Albanese, L.; Ciriminna, R.; Meneguzzo, F.; Pagliaro, M. Gluten reduction in beer by hydrodynamic cavitation assisted brewing of barley malts. *LWT Food Sci. Technol.* **2017**, *82*, 342–353. [CrossRef]
38. CAVIBEER | CNR & Bysea S.r.l. Cavibeer. Available online: http://www.cavibeer.com/ (accessed on 25 July 2019).
39. Albanese, L.; Baronti, S.; Liguori, F.; Meneguzzo, F.; Barbaro, P.; Vaccari, F.P. Hydrodynamic cavitation as an energy efficient process to increase biochar surface area and porosity: A case study. *J. Clean. Prod.* **2019**, *210*, 159–169. [CrossRef]
40. Albanese, L.; Ciriminna, R.; Meneguzzo, F.; Pagliaro, M. Energy efficient inactivation of Saccharomyces cerevisiae via controlled hydrodynamic cavitation. *Energy Sci. Eng.* **2015**, *3*, 221–238. [CrossRef]
41. Carpenter, J.; George, S.; Saharan, V.K. Low pressure hydrodynamic cavitating device for producing highly stable oil in water emulsion: Effect of geometry and cavitation number. *Chem. Eng. Process. Process Intensif.* **2017**, *116*, 97–104. [CrossRef]
42. Ciriminna, R.; Albanese, L.; Meneguzzo, F.; Pagliaro, M. Hydrogen Peroxide: A key chemical for today's sustainable development. *ChemSusChem* **2016**, *9*, 3374–3381. [CrossRef]
43. Yusaf, T.; Al-Juboori, R.A. Alternative methods of microorganism disruption for agricultural applications. *Appl. Energy* **2014**, *114*, 909–923. [CrossRef]

44. Yan, Y.; Thorpe, R.B. Flow regime transitions due to cavitation in the flow through an orifice. *Int. J. Multiph. Flow* **1990**, *16*, 1023–1045. [CrossRef]
45. Bagal, M.V.; Gogate, P.R. Wastewater treatment using hybrid treatment schemes based on cavitation and Fenton chemistry: A review. *Ultrason. Sonochem.* **2014**, *21*, 1–14. [CrossRef] [PubMed]
46. Gogate, P.R. Cavitation: An auxiliary technique in wastewater treatment schemes. *Adv. Environ. Res.* **2002**, *6*, 335–358. [CrossRef]
47. Šarc, A.; Kosel, J.; Stopar, D.; Oder, M.; Dular, M. Removal of bacteria *Legionella pneumophila*, *Escherichia coli*, and *Bacillus subtilis* by (super)cavitation. *Ultrason. Sonochem.* **2018**, *42*, 228–236. [CrossRef] [PubMed]
48. King, A.J.; Dickinson, J.R. Biotransformation of hop aroma terpenoids by ale and lager yeasts. *FEMS Yeast Res.* **2003**, *3*, 53–62. [CrossRef] [PubMed]
49. Dickinson, J.R. Terpenoids in Beer. In *Beer in Health and Disease Prevention*; Preedy, V.R., Ed.; Academic Press: San Diego, CA, USA, 2009; pp. 327–332. ISBN 9780123738912.
50. Angelidaki, I.; Alves, M.; Bolzonella, D.; Borzacconi, L.; Campos, J.L.; Guwy, A.J.; Kalyuzhnyi, S.; Jenicek, P.; Van Lier, J.B. Defining the biomethane potential (BMP) of solid organic wastes and energy crops: A proposed protocol for batch assays. *Water Sci. Technol.* **2009**, *59*, 927–934. [CrossRef] [PubMed]
51. Buswell, A.M.; Mueller, H.F. Mechanism of methane fermentation. *Ind. Eng. Chem.* **1952**, *44*, 550–552. [CrossRef]
52. Mohnen, D. Pectin structure and biosynthesis. *Curr. Opin. Plant Biol.* **2008**, *11*, 266–277. [CrossRef]
53. Morra, M.; Cassinelli, C.; Cascardo, G.; Nagel, M.D.; Della Volpe, C.; Siboni, S.; Maniglio, D.; Brugnara, M.; Ceccone, G.; Schols, H.A.; Ulvskov, P. Effects on interfacial properties and cell adhesion of surface modification by pectic hairy regions. *Biomacromolecules* **2004**, *5*, 2094–2104. [CrossRef]
54. Morris, G.A.; Foster, T.J.; Harding, S.E. The effect of the degree of esterification on the hydrodynamic properties of citrus pectin. *Food Hydrocoll.* **2000**, *14*, 227–235. [CrossRef]
55. McConaughy, S.D.; Stroud, P.A.; Boudreaux, B.; Hester, R.D.; McCormick, C.L. Structural characterization and solution properties of a galacturonate polysaccharide derived from Aloe vera capable of in situ gelation. *Biomacromolecules* **2008**, *9*, 472–480. [CrossRef]
56. Zhao, S.; Yang, F.; Liu, Y.; Sun, D.; Xiu, Z.; Ma, X.; Zhang, Y.; Sun, G. Study of chemical characteristics, gelation properties and biological application of calcium pectate prepared using apple or citrus pectin. *Int. J. Biol. Macromol.* **2018**, *109*, 180–187. [CrossRef] [PubMed]
57. Yang, L.; Kruse, B. Revised Kubelka–Munk theory I theory and application. *J. Opt. Soc. Am. A* **2004**, *21*, 1933. [CrossRef]
58. Khan, M.K.; Abert-Vian, M.; Fabiano-Tixier, A.S.; Dangles, O.; Chemat, F. Ultrasound-assisted extraction of polyphenols (flavanone glycosides) from orange (Citrus sinensis L.) peel. *Food Chem.* **2010**, *119*, 851–858. [CrossRef]
59. Raffa, K.F.; Smalley, E.B. Interaction of pre-attack and induced monoterpene concentrations in host conifer defense against bark beetle-fungal complexes. *Oecologia* **1995**, *102*, 285–295. [CrossRef] [PubMed]
60. Filippov, M.P. IR spectra of pectin films. *J. Appl. Spectrosc.* **1974**, *17*, 1052–1054. [CrossRef]
61. Synytsya, A.; Čopíková, J.; Matějka, P.; Machovič, V. Fourier transform Raman and infrared spectroscopy of pectins. *Carbohydr. Polym.* **2003**, *54*, 97–106. [CrossRef]
62. Chatjigakis, A.K.; Pappas, C.; Proxenia, N.; Kalantzi, O.; Rodis, P.; Polissiou, M. FT-IR spectroscopic determination of the degree of esterification of cell wall pectins from stored peaches and correlation to textural changes. *Carbohydr. Polym.* **1998**, *37*, 395–408. [CrossRef]
63. Assifaoui, A.; Loupiac, C.; Chambin, O.; Cayot, P. Structure of calcium and zinc pectinate films investigated by FTIR spectroscopy. *Carbohydr. Res.* **2010**, *345*, 929–933. [CrossRef]
64. Monsoor, M.A.; Kalapathy, U.; Proctor, A. Improved method for determination of pectin degree of esterification by diffuse reflectance Fourier transform infrared spectroscopy. *J. Agric. Food Chem.* **2001**, *49*, 2756–2760. [CrossRef]
65. Nkhili, E.; Tomao, V.; El Hajji, H.; El Boustani, E.S.; Chemat, F.; Dangles, O. Microwave-assisted water extraction of green tea polyphenols. *Phytochem. Anal.* **2009**, *20*, 408–415. [CrossRef]
66. Albanese, L.; Meneguzzo, F. 7—Hydrodynamic cavitation-assisted processing of vegetable beverages: Review and the case of beer-brewing. In *Production and Management of Beverages*; Grumezescu, A.M., Holban, A.M., Eds.; Woodhead Publishing: Sawston, Cambridge, 2019; pp. 211–257. ISBN 978-0-12-815260-7.

67. Ciriminna, R.; Fidalgo, A.; Delisi, R.; Tamburino, A.; Carnaroglio, D.; Cravotto, G.; Ilharco, L.M.; Pagliaro, M. Controlling the degree of esterification of citrus pectin for demanding applications by selection of the source. *ACS Omega* **2017**, *2*, 7991–7995. [CrossRef] [PubMed]
68. Ciriminna, R.; Meneguzzo, F.; Pagliaro, M. Orange oil. In *Green Pesticides Handbook: Essential Oils for Pest Control*; Nollet, L.M.L., Rathore, H.S., Eds.; CRC Press: Boca Raton, FL, USA, 2017; pp. 291–303. ISBN 978-1-49-875938-0.
69. Maté, J.; Periago, P.M.; Palop, A. When nanoemulsified, d-limonene reduces Listeria monocytogenes heat resistance about one hundred times. *Food Control* **2016**, *59*, 824–828. [CrossRef]
70. Ghasemi, S.; Jafari, S.M.; Assadpour, E.; Khomeiri, M. Production of pectin-whey protein nano-complexes as carriers of orange peel oil. *Carbohydr. Polym.* **2017**, *177*, 369–377. [CrossRef] [PubMed]
71. Ghasemi, S.; Jafari, S.M.; Assadpour, E.; Khomeiri, M. Nanoencapsulation of D-limonene within nanocarriers produced by pectin-whey protein complexes. *Food Hydrocoll.* **2018**, *77*, 152–162. [CrossRef]
72. Wu, Z.; Tagliapietra, S.; Giraudo, A.; Martina, K.; Cravotto, G. Harnessing cavitational effects for green process intensification. *Ultrason. Sonochem.* **2019**, *52*, 530–546. [CrossRef]
73. Razzaghi, S.E.; Arabhosseini, A.; Turk, M.; Soubrat, T.; Cendres, A.; Kianmehr, M.H.; Perino, S.; Chemat, F. Operational efficiencies of six microwave based extraction methods for orange peel oil. *J. Food Eng.* **2019**, *241*, 26–32. [CrossRef]
74. Chemat, F.; Vian, M.A.; Cravotto, G. Green extraction of natural products: Concept and principles. *Int. J. Mol. Sci.* **2012**, *13*, 8615–8627. [CrossRef]